Disorder-induced critical behavior in driven diffusive systems

Bosiljka Tadić*
Jožef Stefan Institute, P.O. Box 3000, 1001 Ljubljana, Slovenia
(Received 27 February 1998)

Using a dynamic renormalization group, we study the transport in driven diffusive systems in the presence of a quenched, random drift velocity with long-range correlations along the transport direction. In dimensions $d < 4$ we find fixed points representing different universality classes of disorder-dominated self-organized criticality and a continuous phase transition at a critical variance of disorder. Numerical values of the scaling exponents characterizing the distributions of relaxation clusters are in good agreement with the exponents measured in natural river networks. [S1063-651X(98)02707-X]

PACS number(s): 64.60.Lx, 05.60.+w, 64.60.Ak, 92.40.Fb

I. INTRODUCTION

Various interacting driven systems self-organize into critical steady states, optimizing in that way their response as a *single functional unit* [1]. An important feature of these systems is their response in the presence of disorder. The effects of disorder on critical properties in steady states have been investigated [2,3] in cellular automata and coarse-grained continuum models. It has been recognized that disorder changes local relaxation rules and breaks some symmetries of the dynamics, which may result in a qualitatively different global dynamic state. A distinct class of physical phenomena in driven systems exhibits the scale-free behavior *only* in the presence of disorder. Examples include energy transport in the integrate-and-fire oscillators with diversity [4] and Barkhausen noise in spatially disordered ferromagnets [5]. Fluctuations of the optimal path in heterogeneous materials [6] and landscape evolution due to river networks flowing in naturally fractal environment [7–9] also belong to this class of dynamical systems.

Most studies of self-organized criticality (SOC) have been done on sandpile automata, in which the nonlinearity responsible for SOC is due to threshold condition of toppling. In the continuum equation of motion for the dynamic variable height $h(\vec{x},t)$, this leads to an infinite series of relevant operators $\mu_n \partial^2 h^n$ [10]. Recent numerical simulations of stochastic automata with a ''soft'' threshold reveal different universality classes of SOC and a phase transition when the probability of toppling is varied [11]. Complementary to numerical simulations, the renormalization group studies of continuum equations are aimed at characterizing the critical behavior at large distances and long times. Hwa and Kardar [12] introduced a transport equation that is compatible with all symmetries of anisotropic flow in open diffusive system, with the leading nonlinearity $\lambda \partial_\parallel h^2$ generated by nonlinear friction.

In this work we study the transport equation of open diffusive systems in the presence of quenched random drift velocity. We adopt an anisotropic d-dimensional model for the height $h(\vec{x},t)$ transport with Hwa-Kardar (HK) nonlinearity $\lambda \partial_\parallel h^2$ and introduce quenched disorder via a term $p(x)\partial_\parallel h$, which locally breaks the joint inversion symmetry $h \to -h$, $x_\parallel \to -x_\parallel$. The symmetry is globally restored by assuming the distribution of disorder with zero mean, which thus excludes the global current through the system. We also consider long-range correlations of disorder along the direction of transport varying with distance as $\sim \gamma x_\parallel^{-2+\delta}$ and a weak (anti)correlation in the perpendicular direction (see below). In our model $p(x)$ represents the spatially varying local velocity of profile fluctuations, which is motivated by mass transport in realistic granular and river flow with a preferred direction of drainage. It should be stressed that our model differs from continuum models of SOC studied so far both in its symmetry properties and in correlations of defects. Meanwhile, in models of randomly driven interfaces [13] a similar disorder term appears in a physically different context.

Using a dynamic renormalization group in the hydrodynamic (HD) limit, we show that this type of disorder represents a relevant perturbation in dimensions $d \leqslant 4$, leading to a different disorder-induced scaling behavior. We calculate the critical exponents at fixed points in the $\epsilon \equiv 4-d$ and δ expansions to leading order [14]. It is interesting to note that in the absence of disorder the ϵ expansion to leading order yields the exact critical exponents in the HD limit, as discussed in detail in Ref. [12]. Using scaling arguments eligible for directed dynamic processes that generate self-affine structures, we also determine the avalanche exponents in terms of the anisotropy exponent.

The organization of the paper is as follows. In Sec. II we introduce the stochastic differential equation with disorder and discuss our motivation for the long-range disorder correlations. In Sec. III the details of the dynamic renormalization group analysis are given. In Sec. IV we discuss the critical behavior at disorder-induced fixed points for various physical values of the parameters and their relevance for the problems of river networks and strongly disordered dynamical systems. A short summary of the results is given in Sec. V.

II. STOCHASTIC EQUATION OF DISORDER-DOMINATED NETWORKS

We start with the anisotropic diffusion equation for the height transport [12] with nonlinear friction

*Electronic address: Bosiljka.Tadic@ijs.si

$$\frac{\partial h}{\partial t}=\nu_{\parallel}\partial_{\parallel}^{2}h+\nu_{\perp}\partial_{\perp}^{2}h-\frac{\lambda}{2}\partial_{\parallel}h^{2}-p(x)\partial_{\parallel}h+\eta \qquad (1)$$

and a time-dependent *nonconserving* Langevin force

$$\langle \eta(x,t)\,\eta(x',t')\rangle=2D\,\delta^{(d)}(x-x')\,\delta(t-t'). \qquad (2)$$

The random term proportional to $p(x)$ locally breaks joint inversion symmetry, which is obeyed by the remaining terms [12]. We assume the distribution of $p(x)$ as

$$\langle p(x)\rangle_{d}=0, \quad \langle p(x)p(x')\rangle_{d}=\gamma f(x-x'), \qquad (3)$$

with $f(x)=x_{\parallel}^{-a}\;x_{\perp}^{c}$. For consistency of the perturbation expansion (see below) we choose $a=2-\delta$ and $c\sim O(2-z)$. In Eq. (1) anisotropy signals the existence of a preferred direction of mass flow, which is the subject of two nonlinear terms $(\lambda/2)(\partial_{\parallel}h^{2})$ and $\gamma f(x)(\partial_{\parallel}h)^{2}$. The motivation for long-range disorder correlations is as follows. We assume that Eqs. (1)–(3) describe the evolution of heights (e.g., of a granular pile or landscape), which eventually leads to a self-organized structured landscape with a network of channels, along which the material is being eroded. It is important to keep in mind that these channels appear dynamically as a result of diffusion, which is influenced by an interplay of the above two nonlinear terms. Therefore, an initial configuration that is based mainly on the configuration of disorder helps to imprint the channels by setting locally most probable drift paths. However, since the system is open and repeatedly perturbed by the nonconserving noise η, the once established network of channels is likely to evolve under further perturbations, reaching a new stationary configuration, in which effects of disorder are altered. An example of dynamically modified disorder effects can be found in the field-driven random Ising model, in which pinning by local random fields appears weakened by sweeping an avalanche of flipped spins over certain pinning centers. The size of an avalanche is the subject of the dynamics itself. Another interesting example is represented by erosion of natural landscapes due to water flow. In the course of evolution, the originally preferred local drift directions become uneffective at sites that are found inside the correlated area that already drains to a different direction. Observations in natural river basins reveal [15,16] a persistent correlation between the average soil slope at a site x and area $s(x)$ that drains to that point as $\nabla h(x)\sim[s(x)]^{-1/2}$. Here the drainage area $s(x)$ is not fixed but is determined self-consistently by the dynamics itself. A nice example of this relation at work is shown in Ref. [16], where a procedure numerically iterated to *self-consistency* yields a self-similar river network. In the stationary critical state we have $s(x)\sim x_{\parallel}^{D_{\parallel}}\phi(x_{\perp}/x_{\parallel}^{\zeta})$, where $D_{\parallel}$ is the fractal dimension with respect to parallel length and ζ is the anisotropy exponent (see below). It is reasonable to assume that for $x_{\parallel}\to\infty$ the scaling function $\phi(r)$ behaves as a power of r, i.e., $\phi(r)\sim r^{\eta}$. Therefore, for the *intermittent* dynamic regime [where eroded material from the area $s(x)$ is accumulated at point x building up a shear stress $\sigma(x)$ and erupting when the stress exceeds a critical value σ_{c}], the leading nonlinear term is proportional to $\sim(\nabla h)^{2}/x_{\parallel}^{D_{\parallel}-\eta\zeta}x_{\perp}^{\eta}$.

In order to mimic the above processes in which the effects of disorder are being dynamically modified, we only fix the disorder correlations in the direction of transport. The transverse correlations are then determined self-consistently by the fluctuations in the critical steady state [17]. Notice that the difference $2-z$ is a measure of the strength of critical fluctuations (see Sec. III).

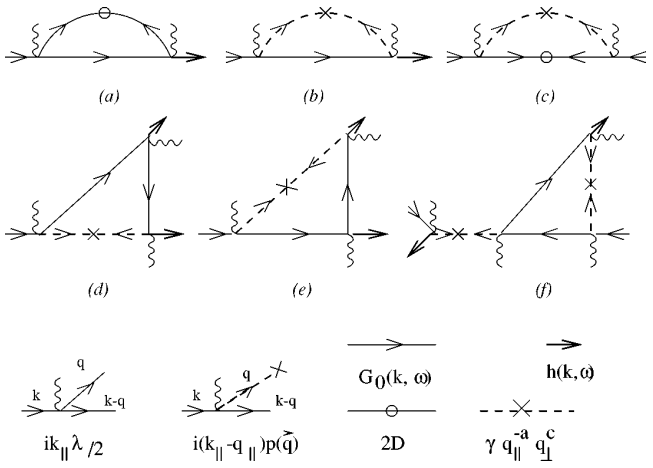

FIG. 1. One-loop diagrams with nonzero contributions to (a) and (b) the renormalized propagator, (c) dynamic noise D, and vertices (d) and (e) $\lambda/2$ and (f) γ. The symbols are defined in the bottom line.

III. DYNAMIC RENORMALIZATION GROUP ANALYSIS

The dynamic renormalization group consists of eliminating fast modes with subsequent rescaling: $t\to b^{z}t$, $x_{\parallel}\to bx_{\parallel}$, $x_{\perp}\to b^{\zeta}x_{\perp}$, and $h\to b^{\chi}h$, where z, ζ, and χ are the dynamic, anisotropy, and roughness exponents, respectively. Naive dimensions of the coupling constants in Eq. (1) are then obtained from the scaled equation

$$\partial h/\partial t=b^{z-2}\nu_{\parallel}\partial_{\parallel}^{2}h+b^{z-2\zeta}\nu_{\perp}\partial_{\perp}^{2}h-b^{z+\chi-1}\frac{\lambda}{2}\partial_{\parallel}h^{2}$$
$$+b^{z-1+\mu_{p}}p(x)\partial_{\parallel}h+b^{z-\chi+\mu_{\eta}}\eta,$$

where, according to Eqs. (2) and (3), we have $\mu_{p}=-\frac{1}{2}(a-c\zeta)$ and $\mu_{\eta}=-\frac{1}{2}[1+\zeta(d-1)+z]$. In $(\vec{k},\omega)$ space the equation of motion becomes

$$h(\vec{k},\omega)=G_{0}(\vec{k},\omega)\Bigg[\eta(\vec{k},\omega)-ik_{\parallel}\frac{\lambda}{2}\int\frac{d^{d}q}{(2\pi)^{d}}\frac{d\omega'}{2\pi}h(\vec{q},\omega')$$
$$\times h(\vec{k}-\vec{q},\omega-\omega')-i\int\frac{d^{d}q}{(2\pi)^{d}}\frac{d\omega'}{2\pi}(k_{\parallel}-q_{\parallel})$$
$$\times p(\vec{q})h(\vec{k}-\vec{q},\omega-\omega')\Bigg], \qquad (4)$$

with the propagator $G_{0}(\vec{k},\omega)=\nu_{\parallel}k_{\parallel}^{2}+\nu_{\perp}k_{\perp}^{2}-i\omega$. Iterating Eq. (4) and eliminating fast modes leads to a diagrammatic expansion (see Fig. 1). In the HD limit $k_{\perp}\to0$, $\omega\to0$, $k_{\parallel}\ll1$, keeping the lowest respective orders of $k_{\parallel}$, we calculate the one-loop contributions to the recursion relations [$\ell\equiv\ln b$, $S_{d}=2^{1-d}\pi^{-d/2}/\Gamma(d/2)$]:

TABLE I. Scaling exponents at fixed points R and M to leading order in the ϵ and δ expansions. Also listed are the mean-field exponents at fixed point G and the exact HK results at fixed point P.

Fixed point	z	ζ	$-\chi$	α	τ
G	2	1	1	2	3/2
P	$\frac{6}{7-d}$	$\frac{3}{7-d}$	$\frac{d-1}{7-d}$	$\frac{10-d}{7-d}$	$\frac{13-d}{10-d}$
M	$2-\frac{3\delta+2\epsilon}{9}$	$1-\frac{3\delta+2\epsilon}{18}$	$1-\frac{2\epsilon}{3}$	$2-\frac{3\delta+2\epsilon}{18}$	$\frac{3}{2}-\frac{9\delta+6\epsilon}{216}$
R	$2-\frac{2\delta}{3}$	$1-\frac{\delta}{3}$	$1-\frac{\delta}{4}-\frac{\epsilon}{2}$	$2-\frac{\delta}{3}$	$\frac{3}{2}-\frac{\delta}{12}$

$$\frac{d\nu_\parallel}{d\ell}=\nu_\parallel\left[z-2+\frac{3\pi}{32}S_d u+2\pi S_d w\right], \tag{5}$$

$$\frac{dD}{d\ell}=D\left[z-2\chi-(d-1)\zeta-1+\frac{\pi}{2}S_d w\right], \tag{6}$$

$$\frac{d\lambda}{d\ell}=\lambda\left[\frac{z}{4}(7-d)-\frac{3}{2}-\frac{3\pi}{4}S_d w\right], \tag{7}$$

$$\frac{d\gamma}{d\ell}=\gamma[2z-2-a+c\zeta+\pi S_d w]. \tag{8}$$

Here the effective couplings u and w are found to be $u\equiv(\lambda^2 D/\nu_\parallel^3)(\nu_\parallel/\nu_\perp)^{(d-1)/2}$ and $w\equiv(\gamma/\nu_\parallel^2)(\nu_\parallel/\nu_\perp)^{(d-1)/2}$. A few comments are in order. (a) As usual in systems with quenched randomness, the perturbation expansion is made at fixed random noise $p(\vec{q})$ and subsequently the graphs are averaged over the distribution of $p(\vec{q})$ leading to a dashed line with a cross, which carries $\gamma q_\parallel^{-a} q_\perp^c$. All graphs must be *connected* before this step is taken, thus leading at most to one cross-dashed line per loop. Due to the quenched nature of the random noise [cf. Eq. (3)], a loop with a cross-dashed line involves *no* frequency integration. However, averaging over the dynamic noise according to Eq. (2) leads to a circle-solid line with two propagators and a factor $2D$ and an integration over the internal frequency. (b) According to Eq. (4), the wiggly line associated with the vertex $\lambda/2$ carries $ik_\parallel$, with $\vec{k}$ being the momentum of the incoming line, whereas the wiggly line associated with the vertex $p(\vec{q})$ carries the momentum $i(k_\parallel-q_\parallel)$ of the outgoing line. Hence both graphs in Figs. 1(a) and 1(b) for the renormalized propagator are proportional to $i(k_\parallel-q_\parallel)ik_\parallel$ and thus do not contribute to the vertex $\nu_\perp$. Therefore, we have $d\nu_\perp/d\ell=\nu_\perp[z-2\zeta]$, leading to $\zeta=z/2$. This argument is valid to all orders in the HD limit. (c) The additional three graphs for $\lambda/2$ and γ (not shown), which are obtained by replacing the cross-dashed line in Figs. 1(d) and 1(f) with a circle-solid line (there are three such graphs for $\lambda/2$ and three for γ, corresponding to a circle-solid line along one of the three sides of the triangle), however, give a null contribution (same as in Ref. [12]). Similarly, a contribution of the graph for dynamic noise D, which is obtained by replacing the cross-dashed line in Fig. 1(c) by a circle-solid line, vanishes.

On approaching a fixed point, we have from Eq. (6) $\chi=[z(3-d)-2+\pi S_d w]/4$. From Eqs. (7) and (8) we find

$$\frac{du}{d\ell}=u\left[\epsilon-\frac{9\pi}{64}S_d u-\frac{9\pi}{2}S_d w\right], \tag{9}$$

$$\frac{dw}{d\ell}=w\left[\delta-\frac{3\pi}{16}S_d u-3\pi S_d w\right], \tag{10}$$

where the small expansion parameters are $\epsilon\equiv 4-d$ and $\delta\equiv 2-a$ and we have chosen $c=(2-z)/2\equiv 1-\zeta$. Notice that this choice of c is selected by the structure of the true expansion parameters u and w, so that ϵ and δ appear as their anomalous dimensions, respectively. Also, the disorder correlations $f(x_\parallel,x_\perp)$ become isotropic when $\zeta=1$, corresponding to the isotropic transport. It should be stressed that for anisotropic disorder correlations no additional parameters are generated to leading order. Equations (9) and (10) have four fixed points $(u^\star,w^\star)$: G for Gaussian (0,0), P for pure $(64\epsilon/9\pi S_d,0)$, R for random $(0,\delta/3\pi S_d)$, and M for mixed $(32(3\delta-2\epsilon)/9\pi S_d,(4\epsilon-3\delta)/9\pi S_d)$.

From Eq. (5) the dynamic exponent is obtained as

$$z=2-\frac{3\pi}{32}S_d u^\star-2\pi S_d w^\star. \tag{11}$$

Using Eq. (11) and the above scaling relations between z, ζ, and χ, we find the exponents in the ϵ and δ expansions, which are shown in Table I. Also shown are the exponents α and τ for the probability distribution of duration $P(t)\sim t^{-\alpha}$ and size of relaxation clusters $P(s)\sim s^{-\tau}$, which can be expressed in terms of ζ using the following scaling arguments (see also Ref. [8]). For *strictly directional* diffusion, the clusters can be visualized as effectively planar structures with the fractal dimension $D_\parallel=1+\zeta$. The average size of clusters scales as $\langle s\rangle\sim L^{d_\ell}$, where L is the linear system size and $d_\ell=1$ for the self-affine clusters (for which $\zeta<1$). On the other hand, $\langle s\rangle\sim L^{D_\parallel(2-\tau)}$ and the scaling relation $D_\parallel(\tau-1)=\alpha-1$ holds in the steady state. Using these relations, we find $\tau=(1+2\zeta)/(1+\zeta)$ and $\alpha=1+\zeta$.

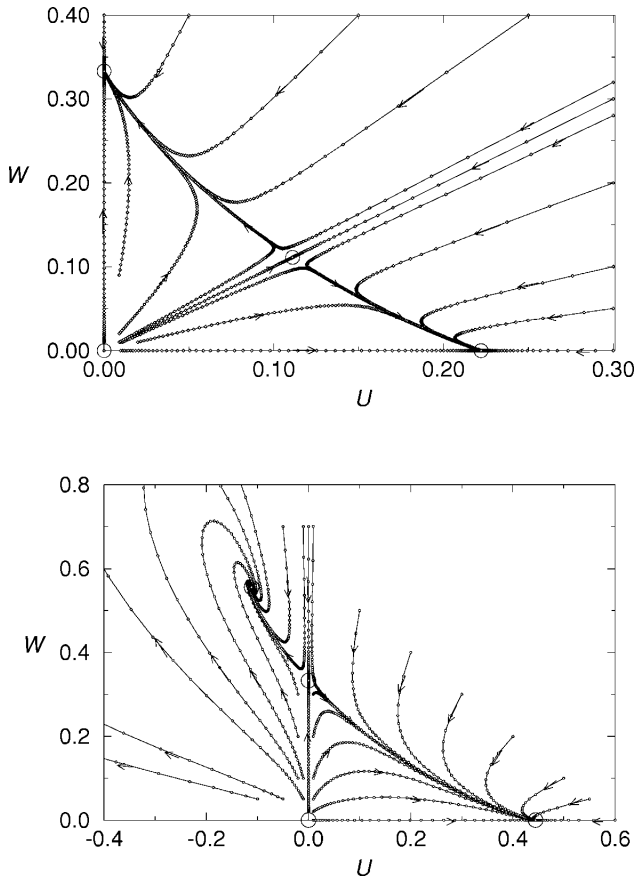

FIG. 2. Flow diagrams for $\delta=1$ and (top) $\epsilon=1$ and (bottom) $\epsilon=2$. Large circles represent fixed points described in the text.

IV. UNIVERSALITY CLASSES OF DISORDER-INDUCED CRITICALITY

As seen from Table I, the fixed point G represents mean-field SOC, which becomes unstable for dimensions $d<4$ with respect to both nonlinearity and disorder. The relative stability of the other three fixed points in the (u,w) plane depends on the parameters ϵ and δ and on the initial value of the ratio w/u. In Fig. 2 we show the flow diagrams of Eqs. (9) and (10) for $\delta=1$ and $\epsilon=1$ and 2. (For convenience we use reduced couplings $U\equiv\pi S_d u/32$ and $W\equiv\pi S_d w$.) In the case $\epsilon=1$, the competition between disorder and the λ term leads to two different types of behavior, which are separated by the line $W/U=1$. The fixed point M, whose domain of attraction is the line $W/U=1$, is unstable in the direction perpendicular to the critical line $W/U=1$, representing a phase transition from pure HK to disorder-controlled SOC with increasing variance of disorder. We find qualitatively the same behavior for short-range correlations ($\delta=2$) in $d=2$. In the case of long-range correlated defects ($\delta=1$) in two dimensions (cf. Fig. 2) the fixed point M moves to the negative-U region and becomes spirally attractive. The entire first quadrant flows towards the pure HK fixed point P. The flow lines are first attracted to a section of the curve connecting the fixed points R and P approaching the fixed point P under a nonzero angle.

Taking the analytic continuation to $\delta\to1$ and $\epsilon\to$ 1 or 2, corresponding to physical $d=$ 2+1 or 1+1 dimensions [18], respectively, we obtain numerical values of the exponents, which are listed in Table II. Here $\delta=1$ was taken as a *typical* example of long-range correlations. Notice that in contrast to ϵ, which is restricted to integer values, the parameter δ may vary continuously in the range $0<\delta<2$. It is noteworthy that the exponents at all three fixed points in $d=2+1$ are close to values measured in natural river networks (RNs). For river basins around the world the exponents are found [7] to be $\tau=1.41-1.45$, $\alpha=1.67-1.92$, $\zeta=0.67-0.92$, and Hack's exponent $h=0.54-0.6$ satisfying the scaling relation $h=1/\alpha$. The roughness exponent for large length scales [19] was found in the range $\chi=0.3-0.55$. Variations in the values of the exponents depend on geographical location where they have been measured and can be related to locally dominated erosion mechanisms [20]. With regard to the results in Table II, we would like to point out the following. (i) In the absence of disorder $\gamma=0$, corresponding to the limit studied by Hwa and Kardar in Ref. [12], the exponents are within the range of the above RN exponents, indicating that the HK model of flowing granular piles captures the basic features of landscape evolution. It should be stressed that in this case ($\gamma=0$) the values of the exponents are exact and are not a subject of higher-order corrections in the perturbation expansion (see Ref. [12] for details). (ii) For finite disorder $\gamma\neq0$ two more fixed points are accessible, depending on the initial values of γ and λ. Therefore, variations of numerical values of the exponents can be attributed to different universality classes, which are accessible for varying initial strengths of disorder. In particular, α decreases from 1.75 at the HK limit to 1.72 at fixed point M and eventually to 1.66 at fixed point R by increasing disorder γ at fixed λ (see Fig. 2, top). In addition, the exponents at fixed points M and R vary with the range of disorder correlations δ (values of δ in the interval $0<\delta<2$ correspond to long-range correlations). For instance, for $\delta=1/3$, $\epsilon=1$ we have at fixed point M $\zeta=0.83$, $\alpha=1.83$, and $\tau=1.45$. It is interesting to note that the same values for cluster exponents are obtained by the numerical procedure in Ref. [16]. According to the discussion in Sec. II, we have that for $\zeta=0.83$ the exponent in the leading nonlinear term becomes $D_{\|}-\zeta(1-\zeta)=1.69$, which is close to $2-\delta=1.67$. On the other hand, for shorter disorder correlations, e.g., for $\delta=3/2$, we find $\alpha=1.64$ and $\tau=1.39$. The importance of disorder for river networks has been also pointed out by Caldarelli *et al.* in Ref. [21], where numerical simulations of a cellular automaton model of randomly pinned landscape evolution yields the exponents very close to those at fixed point M (see Table II). Moreover, in the

TABLE II. Numerical values of the critical exponents at various fixed points for $\delta=1$ and $\epsilon=1$ (first three rows) and $\delta=1$ and $\epsilon=2$ (last three rows).

Fixed point	z	ζ	χ	α	τ	ϵ
P	1.5	0.75	−0.5	1.75	1.428	1
M	1.44	0.72	−0.33	1.72	1.418	1
R	1.33	0.66	−0.25	1.66	1.40	1
P	1.2	0.6	−0.2	1.6	1.375	2
M	1.22	0.62	0.33	1.62	1.371	2
R	1.33	0.66	0.25	1.66	1.40	2

absence of pinning, the same authors [21] found the exponents close to HK fixed point P given in Table II.

At fixed point R, representing the universality class in the strong disorder limit ($\lambda=0$), the exponents are in very good agreement (cf. Table II) with the results of numerical simulations of Ref. [9], suggesting small higher-order corrections ($d_{\not\subset}=0.98\pm0.02$, $\zeta=0.66\pm0.02$, and $\tau=1.40\pm0.02$) for self-affine networks with disorder-dominated basins in two dimensions. It has been argued in the literature [6,9] that the problem of optimal path in strongly disordered medium and Eden growth processes also belong to this universality class. In these systems the disorder effects are dynamically modified. Eden growth is not defined as a disordered problem; however, an effective quenched disorder with long-range correlations is self-generated by the blocking effects of previously occupied sites [see Ref. [6(b)]]. Similarly, in the above-mentioned example of disorder-dominated basins in two dimensions sites that are already connected at time t influence the course of the process at later time steps. In numerical simulations of cellular automata models, such as done in Refs. [9,21,11], for instance, a particular range of disorder correlations is *not specified*. The exponents are measured in the emergent stationary critical state, which is obtained after many successive updates. To our knowledge, a stochastic differential equation for dynamically varying disorder effects in these systems has not been considered so far. Here we argue that Eq. (1) with disorder correlations of the type $f(x)\sim x_{\|}^{-1}x_{\perp}^{1-\zeta}$ might capture the critical properties of these dynamical systems.

Following the general scaling arguments of Ref. [12], we estimate the behavior of the order parameter, defined in analogy to cellular automata by the average outflow current

$$\langle J(W)\rangle=\int\frac{dt}{T}\int d^{d-1}x_{\perp}\,j(L_{\|},x_{\perp},t,W). \tag{12}$$

In the steady state $\langle J(W)\rangle\equiv1$, and exhibiting fluctuations near the transition, hence we have $\langle J(W)\rangle\sim W^{\beta}$. For small disorder the local current is $j\sim h^2$; thus we have $j(L_{\|},x_{\perp},t,W)\sim b^{2\chi}j(b^{-1}L_{\|},b^{-\zeta}x_{\perp},b^{-z}t,b^{-\mu_w}W)$ or $j(L_{\|},x_{\perp},t,W)\sim x_{\perp}^{2\chi/\zeta}\phi(tx_{\perp}^{-z/\zeta},Wx_{\perp}^{-\delta/\zeta})$. Inserting the last expression into Eq. (12) and after extracting formally the W dependence, we find $\beta=[2\chi+\zeta(d-1)]/\delta$. The directed diffusion in our model represents some kind of a contact process; therefore, for $t\to\infty$ and $x_{\|}\to\infty$ the following scaling relation holds: $\beta/\bar{\nu}=\alpha'$. Here $\bar{\nu}$ is the parallel correlation length exponent and $\alpha'\equiv\alpha-1$ is the exponent of the survival probability distribution. At fixed point M for $\delta=1$ and $\epsilon=1$ we find $\beta=0.78$ and $\bar{\nu}=1.08$. A similar value $\beta=0.86$ was found in the stochastic cellular automaton [see Ref. [11(a)]].

V. CONCLUSIONS

We have demonstrated that our transport equation with quenched disorder in the drift velocity with *anisotropic* long-range correlations describes two different universality classes of critical behavior in open diffusive systems. For finite disorder we find SOC relevant for the scaling properties of fractal river networks. For low disorder a crossover to the asymptotic behavior controlled by the HK fixed point occurs [12]. At critical variance of disorder a continuous phase transition occurs between the two different types of steady states: channel-type flow for strong disorder and low friction and surfacelike flow for low disorder and high friction. The comparison of the numerical values of the avalanche exponents at fixed points in $2+1$ dimensions with the exponents measured in natural river networks [7] is quite satisfactory. Our analysis suggests that natural river networks may result from the interplay between quenched disorder and an effective nonlinear friction. Variations in the range of disorder correlations $0<\delta<2$ appear as a possible underlying mechanism that explains the observed variations in the exponents of natural networks. A *distinct* universality class of disorder-induced self-organized criticality is represented by the fixed point R of our model, where $\lambda=0$. Evidence collected by numerical simulations in Refs. [6,9] suggests that a number of other disordered dynamical systems should have the same critical behavior described by the fixed point R. In the present work we pointed out the importance of long-range correlations in this class of self-organizing disordered systems.

ACKNOWLEDGMENTS

This work was supported by the Ministry of Science and Technology of the Republic of Slovenia. I am grateful to Al Corral, Nicolay Antonov, Amos Maritan, and Achille Giacometti for helpful discussions.

[1] P. Bak, *How Nature Works* (Copernicus Springer-Verlag, New York, 1996), and references therein.

[2] B. Tadić, U. Nowak, K. D. Usadel, R. Ramaswamy, and S. Padlewski, Phys. Rev. A **45**, 8536 (1992); B. Tadić and R. Ramaswamy, Physica A **224**, 188 (1996); Phys. Rev. E **54**, 3157 (1996).

[3] J. Toner, Phys. Rev. Lett. **66**, 679 (1991).

[4] A. Corral, C. J. Pérez, and A. Díaz-Guilera, Phys. Rev. Lett. **78**, 1492 (1997).

[5] B. Tadić, Phys. Rev. Lett. **77**, 3843 (1996).

[6] (a) M. Cieplak, A. Maritan, and J. R. Banavar, Phys. Rev. Lett. **72**, 2320 (1994); (b) **76**, 3754 (1996).

[7] R. Rigon, I. Rodrigues-Iturbe, A. Maritan, A. Giacometti, D. G. Tarboton, and A. Rinaldo, Water Resour. Res. **32**, 3367 (1996).

[8] A. Maritan, A. Rinaldo, R. Rigon, A. Giacometti, and I. Rodrigues-Iturbe, Phys. Rev. E **53**, 1510 (1996); A. Maritan, F. Coloari, A. Flamini, M. Cieplak, and J. R. Banavar, Science **272**, 984 (1996).

[9] M. Cieplak, A. Giacometti, A. Maritan, A. Rinaldo, I. Rodrigues-Iturbe, and J. R. Banavar, Phys. Rev. E (to be published).

[10] A. Díaz-Guilera, Phys. Rev. A **45**, 8551 (1992); A. Corral and A. Díaz-Guilera, Phys. Rev. E **55**, 2434 (1997).

[11] (a) S. Lübeck, B. Tadić, and K. D. Usadel, Phys. Rev. E **53**, 2182 (1996); (b) B. Tadić and D. Dhar, Phys. Rev. Lett. **79**, 1519 (1997); (c) B. Tadić, Phys. Rev. E **57**, 4375 (1998).
[12] T. Hwa and M. Kardar, Phys. Rev. Lett. **62**, 1813 (1989); Phys. Rev. A **45**, 7002 (1992).
[13] J. Krug, Phys. Rev. Lett. **75**, 1795 (1995); G. Tripathy and M. Barma, *ibid.* **78**, 3039 (1997).
[14] A double ϵ and δ expansion is used in the study of conventional critical behavior in the presence of long-range correlated disorder: See A. Weinrib and B. I. Halperin, Phys. Rev. B **27**, 413 (1983), and references therein.
[15] L. Leopold, Am. J. Sci. **251**, 606 (1953).
[16] J. R. Banavar, F. Colaiori, A. Flammini, A. Giacometti, A. Maritan, and A. Rinaldo, Phys. Rev. Lett. **78**, 4522 (1997).
[17] Therefore, c is renormalized together with other parameters of the system λ and γ; however, it remains of $O(\epsilon,\delta)$, i.e., in the same part of parameter space, thus ensuring a consistent perturbation expansion.
[18] For dynamic contact processes evolving on an internal time scale d can be identified as $d-1$ spatial dimension and time, similarly to directed percolation.
[19] M. Matsushita and S. Ouchi, Physica D **38**, 246 (1989).
[20] See, for instance, J. D. Pelletier, e-print cond-mat/970533, and references therein.
[21] G. Caldarelli, A. Giacometti, A. Maritan, I. Rodriguez-Iturbe, and A. Rinaldo, Phys. Rev. E **55**, R4865 (1997).